

MULTICHANNEL WIENER FILTER PERFORMANCE ANALYSIS IN PRESENCE OF MISMODELING

Dani Cherkassky

Faculty of Engineering
Bar-Ilan University, Israel
dani.cherkassky@gmail.com

Sharon Gannot

Faculty of Engineering
Bar-Ilan University, Israel
sharon.gannot@biu.ac.il

ABSTRACT

A randomly positioned microphone array is considered in this work. In many applications, the locations of the array elements are known up to a certain degree of random mismatch. We derive a novel statistical model for performance analysis of the multi-channel Wiener filter (MWF) beamformer under random mismatch in sensors location. We consider the scenario of one desired source and one interfering source arriving from the far-field and impinging on a linear array. A theoretical model for predicting the MWF mean squared error (MSE) for a given variation in sensors location is developed and verified by simulations. It is postulated that the probability density function (p.d.f) of the MSE of the MWF obeys Γ distribution. This claim is verified empirically by simulations.

Index Terms— Beamforming, Random Microphone arrays, Multi-Channel Wiener Filter.

1. INTRODUCTION

Beamformers can nowadays be found in a wide range of applications [1], and in particular in speech processing tasks, e.g. localization, tracking and speech enhancement [2]. In recent years, with advances in sensors and digital processors technology, the concept of wireless acoustic sensor network (WASN) with a large number of arbitrarily deployed sensors becomes feasible.

It is well known that data-dependent beamformers outperform their data-independent counterparts in terms of the directivity factor, i.e., spatial resolution [3]. However, data-dependent beamformers are known to be sensitive to deviations from the assumed spatial characteristics of the setup, such as microphones positions, acoustic medium and desired source position [4], [5]. In many applications, the spatial characteristics are not exactly known and can even change over time. Driven by the applicability of large scale microphone networks, the incorporation of statistical models for describing the spatial characteristics of the setup is gaining interest in the signal processing community. The use of statistical models in array processing was first proposed by Lo [6]. In this seminal contribution the mean beampattern of data-independent arrays was analyzed. Recently, a theoretical analysis of the performance of data-dependent beamformers with random layouts has been proposed by Markovich-Golan et al. [7]. Doclo and Moonen [8] proposed design procedures for improving the mean and worst-case performance of superdirective beamformers in mismatch conditions.

In the current contribution the performance of the MWF beamformer for a linear microphone array with random mismatch in microphones positions is derived. A MWF beamformer is considered due to its applicability to speech processing applications and

its relevance to statistical analysis which is carried out in the sequel. We consider a simplified scenario of a coherent wide-band desired source and a coherent wide-band interfering source arriving from the far-field and impinging on the microphone array, in a non-reverberant environment [9], and corrupted by a spatially-white noise (microphones self-noise). This scenario may be relevant in outdoor speech processing applications such as border security control and wildlife habitat monitoring [10]. For a more common, indoor applications, as conference system, a reverberant model should be considered, which is out of the scope of the current paper and will be considered in a future work.

The rest of the paper is organized as follows. In Sec. 2, the problem is formulated. In Sec. 3, an expression for MSE of the MWF, given the *actual* microphones locations, is derived. Then, in Sec. 4 the statistics of the MMSE is analyzed. The derived theoretical models are empirically verified in Sec. 5. Finally, a discussion is given in Sec. 6.

2. PROBLEM FORMULATION

Consider a coherent wideband desired source and a coherent wide-band interfering source impinging on a M microphone array. The microphone signals are further corrupted by a spatially white noise. In the short-time Fourier transform (STFT) domain, the desired source is denoted $s_d(l, k)$, the interfering source is denoted $s_i(l, k)$ and the sensor noise at the p th microphone is denoted $n_p(l, k)$, where l is the frame index, and k is the frequency index. The analysis window length is denoted N_{DFT} . In the following, the term *nominal* will correspond to values used for designing the beamformer, while the term *actual* will correspond to true values of the received signals:

$$\mathbf{z}_n(l, k) = \mathbf{a}_n^d s_d(l, k) + \mathbf{a}_n^i s_i(l, k) + \mathbf{n}(l, k) \quad (1a)$$

$$\mathbf{z}_a(l, k) = \mathbf{a}_a^d s_d(l, k) + \mathbf{a}_a^i s_i(l, k) + \mathbf{n}(l, k) \quad (1b)$$

where $\mathbf{n}(l, k)$ is a spatially-white sensor noise; \mathbf{a}_n^d and \mathbf{a}_n^i are the nominal desired source and the interfering source steering vectors, respectively; and \mathbf{a}_a^d and \mathbf{a}_a^i are the actual manifolds of the desired source and the interfering source, respectively. The k th wavelength corresponding to the k th frequency index is $\lambda_k = \frac{2c}{f_s} \frac{N_{\text{DFT}}}{k}$, where f_s is the sampling frequency and c is the sound velocity in the medium. The MWF is designed to enhance the desired source component in (1a). However, due to mismodeling, the actual measurements obey (1b). Our goal in this contribution is to analyze the statistical properties of the performance of the MWF in this scenario. The analysis can be carried out for each frequency bin k independently, omitted hereafter for brevity. Denote the total nominal interference

component $\mathbf{v}_n(l) = \mathbf{a}_n^i s_i(l) + \mathbf{n}(l)$. The output of the beamformer \mathbf{w} is given by $y(l) = \mathbf{w}^H \mathbf{z}_a(l)$. MWF is the beamformer that minimizes $J = E \{ |s_d(l) - y(l)|^2 \}$, $\forall l$ and is given by [3]:

$$\mathbf{w}_{\text{mwf}} = \Phi_{\mathbf{z}_n \mathbf{z}_n}^{-1} \phi_{\mathbf{z}_n s_d} \quad (2)$$

where:

$$\Phi_{\mathbf{z}_n \mathbf{z}_n} = E \{ \mathbf{z}_n \mathbf{z}_n^H \} = \sigma_d^2 \mathbf{a}_n^d (\mathbf{a}_n^d)^H + \Phi_{\mathbf{v}_n \mathbf{v}_n} \quad (3a)$$

$$\phi_{\mathbf{z}_n s_d} = E \{ \mathbf{z}_n s_d^* \} = \sigma_d^2 \mathbf{a}_n^d \quad (3b)$$

$$\Phi_{\mathbf{v}_n \mathbf{v}_n} = E \{ \mathbf{v}_n (\mathbf{v}_n)^H \} = \sigma_i^2 \mathbf{a}_n^i (\mathbf{a}_n^i)^H + \sigma_n^2 \mathbf{I}_{M \times M}. \quad (3c)$$

$\sigma_d^2, \sigma_i^2, \sigma_n^2$ are the spectra of the desired source, the interfering source and the microphones self-noise, respectively, and \mathbf{I} is the $M \times M$ identity matrix.

3. MSE ANALYSIS FOR GIVEN ACTUAL MANIFOLDS

In the following section we will analyze the MSE of the MWF calculated using (2), for a given actual manifolds \mathbf{a}_a^d , and \mathbf{a}_a^i , usually different from the nominal manifolds \mathbf{a}_n^d , \mathbf{a}_n^i .

Applying the Woodbury identity to (3a) and substituting the result together with (3b) in (2) yields an explicit expression for the nominal \mathbf{w}_{mwf} :

$$\mathbf{w}_{\text{mwf}}^n = \frac{1}{1/\sigma_d^2 + \alpha} \Phi_{\mathbf{v}_n \mathbf{v}_n}^{-1} \mathbf{a}_n^d \quad (4)$$

where:

$$\Phi_{\mathbf{v}_n \mathbf{v}_n}^{-1} = \frac{1}{\sigma_n^2} \cdot [\mathbf{I}_{M \times M} - \gamma \cdot \mathbf{a}_n^i (\mathbf{a}_n^i)^H] \quad (5a)$$

$$\alpha \triangleq (\mathbf{a}_n^d)^H \Phi_{\mathbf{v}_n \mathbf{v}_n}^{-1} \mathbf{a}_n^d \in \mathbb{R} \quad (5b)$$

$$\gamma \triangleq \frac{\sigma_i^2}{\sigma_n^2 + M \cdot \sigma_i^2}. \quad (5c)$$

The explicit form of $\Phi_{\mathbf{v}_n \mathbf{v}_n}^{-1}$ in (5a) is obtained by applying the Woodbury identity to (3c). Once the \mathbf{w}_{mwf} is set (4), its performance in the nominal scenario (i.e. $\mathbf{z}_n(l) = \mathbf{z}_a(l)$) are well-known in the literature [3], and are given by:

$$\begin{aligned} J_{\text{opt}}(\mathbf{w}_{\text{mwf}}^n) &= \sigma_d^2 - (\mathbf{w}_{\text{mwf}}^n)^H \cdot \Phi_{\mathbf{z}_n \mathbf{z}_n} \cdot \mathbf{w}_{\text{mwf}}^n \\ &= \left[\frac{1}{\sigma_d^2} + \frac{1}{\sigma_n^2} \left(M - \gamma \cdot \left| (\mathbf{a}_n^d)^H \mathbf{a}_n^i \right|^2 \right) \right]^{-1}. \end{aligned} \quad (6)$$

We are interested in analyzing $\mathbf{w}_{\text{mwf}}^n$ performance in miss-modeling conditions, i.e. when the nominal beamformer is applied to the actual signals:

$$J_a(\mathbf{w}_{\text{mwf}}^n) = E \left\{ |s_d - (\mathbf{w}_{\text{mwf}}^n)^H \mathbf{z}_a|^2 | \mathbf{a}_a^d, \mathbf{a}_a^i \right\}. \quad (7)$$

Substituting (4) and (1b) in (7), using $E \{ s_d(l) \mathbf{v}_a \} = 0$ and straight-forward Algebra, the $\mathbf{w}_{\text{mwf}}^n$ MSE in a miss-modeling conditions (i.e. $\mathbf{z}_n(l) \neq \mathbf{z}_a(l)$) can be explicitly written as:

$$\begin{aligned} J_a(\mathbf{w}_{\text{mwf}}^n) &= \sigma_d^2 - \frac{2\sigma_d^2}{1/\sigma_d^2 + \alpha} \Re(\rho_d) + \frac{\sigma_d^2}{(1/\sigma_d^2 + \alpha)^2} |\rho_d|^2 + \\ &+ \frac{\sigma_i^2}{(1/\sigma_d^2 + \alpha)^2} |\rho_{id}|^2 + \frac{\sigma_n^2}{(1/\sigma_d^2 + \alpha)^2} \beta \end{aligned} \quad (8)$$

where:

$$\rho_d \triangleq (\mathbf{a}_a^d)^H \Phi_{\mathbf{v}_n \mathbf{v}_n}^{-1} \mathbf{a}_n^d \in \mathbb{C} \quad (9a)$$

$$\rho_{id} \triangleq (\mathbf{a}_a^i)^H \Phi_{\mathbf{v}_n \mathbf{v}_n}^{-1} \mathbf{a}_n^d \in \mathbb{C} \quad (9b)$$

$$\beta \triangleq (\mathbf{a}_n^d)^H \Phi_{\mathbf{v}_n \mathbf{v}_n}^{-1} \underbrace{\Phi_{\mathbf{v}_n \mathbf{v}_n}^{-1} \mathbf{a}_n^d}_{\mathbf{b}} = \mathbf{b}^H \mathbf{b} \in \mathbb{R} \quad (9c)$$

4. THE STATISTICS OF THE $J_a(\mathbf{w}_{\text{mwf}}^n)$

We will derive now an approximated statistical model for the residual error $J_a(\mathbf{w}_{\text{mwf}}^n)$. We will show that the resulting expression depends on the mismatch between the nominal manifolds and the actual manifolds. Note that (8) depends on the mismatch only through ρ_d and ρ_{id} . All other variables depend on the nominal values.

Denote θ_d and θ_i the desired source and the interfering source directions of arrival, respectively. Assume that the mismatch between the nominal and the actual manifolds results from an uncertainty in microphones locations. The nominal location of the p th microphone $\boldsymbol{\eta}_p$ is given by (10a), where Δ_x and Δ_y are the distances between neighboring sensors on x and y axes, respectively. We assume, without loss of generality, that the microphones' inter-distances are equal. The actual location of the p th microphone \mathbf{r}_p is given by (10b) with $\boldsymbol{\mu}_p$ being the uncertainty in microphones location obeying the Gaussian distribution defined in (10c).

$$\boldsymbol{\eta}_p \triangleq [\eta_p^x, \eta_p^y]^T = [p \cdot \Delta_x, p \cdot \Delta_y]^T \quad (10a)$$

$$\mathbf{r}_p \triangleq [\eta_p^x + \mu_p^x, \eta_p^y + \mu_p^y]^T = \boldsymbol{\eta}_p + \boldsymbol{\mu}_p \quad (10b)$$

$$\boldsymbol{\mu}_p \sim \mathcal{N}(0, \sigma^2 \mathbf{I}_{2 \times 2}). \quad (10c)$$

Using the above definitions, the nominal and the actual manifolds can be explicitly written as:

$$\mathbf{a}_n^d = \left[e^{-j\boldsymbol{\eta}_1^T \boldsymbol{\zeta}_d / \lambda_k}, e^{-j\boldsymbol{\eta}_2^T \boldsymbol{\zeta}_d / \lambda_k}, \dots, e^{-j\boldsymbol{\eta}_M^T \boldsymbol{\zeta}_d / \lambda_k} \right]^T \quad (11a)$$

$$\mathbf{a}_a^d = \left[e^{-j\mathbf{r}_1^T \boldsymbol{\zeta}_d / \lambda_k}, e^{-j\mathbf{r}_2^T \boldsymbol{\zeta}_d / \lambda_k}, \dots, e^{-j\mathbf{r}_M^T \boldsymbol{\zeta}_d / \lambda_k} \right]^T \quad (11b)$$

$$\mathbf{a}_n^i = \left[e^{-j\boldsymbol{\eta}_1^T \boldsymbol{\zeta}_i / \lambda_k}, e^{-j\boldsymbol{\eta}_2^T \boldsymbol{\zeta}_i / \lambda_k}, \dots, e^{-j\boldsymbol{\eta}_M^T \boldsymbol{\zeta}_i / \lambda_k} \right]^T \quad (11c)$$

$$\mathbf{a}_a^i = \left[e^{-j\mathbf{r}_1^T \boldsymbol{\zeta}_i / \lambda_k}, e^{-j\mathbf{r}_2^T \boldsymbol{\zeta}_i / \lambda_k}, \dots, e^{-j\mathbf{r}_M^T \boldsymbol{\zeta}_i / \lambda_k} \right]^T \quad (11d)$$

where

$$\boldsymbol{\zeta}_d \triangleq 2\pi [\cos \theta_d, \sin \theta_d]^T, \quad \boldsymbol{\zeta}_i \triangleq 2\pi [\cos \theta_i, \sin \theta_i]^T. \quad (12)$$

Explicit dependence of ρ_d and ρ_{id} on the uncertainty parameter $\boldsymbol{\mu}_p$ can be derived now. This dependence is revealed by substituting (5a) and (11a)-(11d) in (9a) and (9b). The rather lengthy but straightforward procedure, omitted here for the sake of brevity, results in the following expressions:

$$\rho_d = \frac{1}{\sigma_n^2} \left(\sum_{l=1}^M e^{j\epsilon_l^d} - \gamma \sum_{l=1}^M e^{j\epsilon_l^d} \sum_{p=1}^M e^{ju(p-l)} \right) \quad (13)$$

$$\rho_{id} = \frac{1}{\sigma_n^2} \left(\sum_{l=1}^M e^{j(u_l + \epsilon_l^i)} - \gamma \sum_{l=1}^M e^{j\epsilon_l^i} \sum_{p=1}^M e^{jup} \right) \quad (14)$$

where:

$$\begin{aligned} u &\triangleq \frac{\Delta_x (\cos \theta_i - \cos \theta_d) + \Delta_y (\sin \theta_i - \sin \theta_d)}{\lambda_k / 2\pi} \\ \epsilon_l^d &\triangleq \boldsymbol{\mu}_l^T \boldsymbol{\zeta}_d / \lambda_k \sim \mathcal{N} \left(0, \sigma_\epsilon^2 = \frac{4\pi^2 \sigma^2}{\lambda_k^2} \right) \\ \epsilon_l^i &\triangleq \boldsymbol{\mu}_l^T \boldsymbol{\zeta}_i / \lambda_k \sim \mathcal{N} \left(0, \sigma_\epsilon^2 = \frac{4\pi^2 \sigma^2}{\lambda_k^2} \right). \end{aligned}$$

Similarly, explicit expression for α and β can be obtained by substituting (5a) and (11a)-(11d) in (5b) and (9c), respectively. Again, a straightforward procedure results in the following expressions:

$$\alpha = \frac{1}{\sigma_n^2} \left(M - \frac{1}{\gamma} \sum_{l=1}^M e^{-j\mathbf{u}l} \sum_{p=1}^M e^{j\mathbf{u}p} \right) \quad (15)$$

$$\beta = \frac{1}{\sigma_n^2} \left(\mathbf{a}_n^d - \gamma \mathbf{a}_n^i \sum_{p=1}^M e^{j\mathbf{u}p} \right)^H \left(\mathbf{a}_n^d - \gamma \mathbf{a}_n^i \sum_{p=1}^M e^{j\mathbf{u}p} \right). \quad (16)$$

We will apply now several approximations and simplifications in order to assess the statistics of ρ_d and ρ_{id} . The following assumptions, as described in (A.1)-(A.3), are necessary for simplifying the analysis.

$$\frac{\sigma_n^2}{\sigma_i^2} \ll M \quad (\text{A.1}) \quad \frac{2\pi}{u} \ll M \quad (\text{A.2}) \quad \epsilon_l^i \ll u \quad (\text{A.3})$$

Practically, (A.1) dictates sufficient interference to noise ratio (INR). Under this condition γ , as defined in (5c), can be approximated by $\frac{1}{M}$. Assumption (A.2) requires that angular distance (in wavelengths), as reflected by the array, between the desired and interfering sources is large with respect to the amount of available sensors. When Assumption (A.2) is valid, the summations in (13)-(16) which do not include random elements are vanishing. Assumption (A.3) is limiting the analysis to *small errors*, i.e. the uncertainty in the microphones locations is much smaller than the angular distance, as reflected by the array, between the desired and the interfering sources.

Hereinafter, an analysis under Assumptions (A.1)-(A.3) is carried out. We are able to significantly simplify the expressions for $\rho_d, \rho_{id}, \alpha$ and β which will allow us to analyze the statistical behavior of (8). This will be demonstrated in the sequel.

$$\gamma \sum_{p=1}^M e^{j\mathbf{u}(p-1)} \stackrel{(\text{A.1})}{\approx} \frac{e^{-j\mathbf{u}l}}{M} \sum_{p=1}^M (\cos \mathbf{u}p + j \sin \mathbf{u}p) \stackrel{(\text{A.2})}{\approx} 0 \quad (17a)$$

$$\sum_{l=1}^M e^{j(\mathbf{u}l + \epsilon_l^i)} \stackrel{(\text{A.3})}{\approx} \sum_{l=1}^M (\cos \mathbf{u}l + j \sin \mathbf{u}l) \stackrel{(\text{A.2})}{\approx} 0. \quad (17b)$$

Denote $\tilde{J}_a(\mathbf{w}_{\text{mwf}}^n)$, an approximation of $J_a(\mathbf{w}_{\text{mwf}}^n)$ under (A.1)-(A.3), our goal is to derive the probability density function of \tilde{J}_a . The expression for \tilde{J}_a is obtained by applying (17a) and (17b) to (13)-(16) and substituting the simplified terms in (8):

$$\begin{aligned} \tilde{J}_a(\mathbf{w}_{\text{mwf}}^n) &\triangleq \sigma_d^2 - \frac{2\sigma_d^4}{\sigma_n^2 + M\sigma_d^2} \cdot X + \frac{\sigma_d^6}{(\sigma_n^2 + M\sigma_d^2)^2} \cdot X^2 + \\ &+ \frac{\sigma_d^6}{(\sigma_n^2 + M\sigma_d^2)^2} \cdot Y^2 + \frac{M\sigma_d^4\sigma_n^2}{(\sigma_n^2 + M\sigma_d^2)^2} \end{aligned} \quad (18)$$

where $X \triangleq \sum_{l=1}^M \cos \epsilon_l^d$ and $Y \triangleq \sum_{l=1}^M \sin \epsilon_l^d$ are random variables (RV). Now, since $\{\epsilon_l^d\}_{l=1}^M$ are independent identically distributed RVs, according to the Central Limit Theorem X and Y converge to a Gaussian RV for $M \gg 1$, with expected values μ_X, μ_Y

and variances σ_X^2, σ_Y^2 , respectively. We will calculate these moments now. Due to space constraints only the derivation of the moments of X are presented. The respective quantities of Y can be calculated in a similar way.

$$\begin{aligned} \mu_X &= E \left\{ \sum_{l=1}^M \cos \epsilon_l^d \right\} = \sum_{l=1}^M \Re \left(E \left\{ e^{j\epsilon_l^d} \right\} \right) = \sum_{l=1}^M \Re (\varphi_\epsilon(1)) = \\ &= M \cdot e^{-0.5\sigma_\epsilon^2} \\ \sigma_X^2 &= E \left\{ \left(\sum_{l=1}^M \cos \epsilon_l^d \right)^2 \right\} - M^2 e^{-\sigma_\epsilon^2} = -M^2 e^{-\sigma_\epsilon^2} + \\ &+ E \left\{ \sum_{l=1}^M \left(\Re \left(e^{j\epsilon_l^d} \right) \right)^2 + 2 \sum_{l=1}^{M-1} \sum_{p=l+1}^M \Re \left(e^{j\epsilon_l^d} \right) \Re \left(e^{j\epsilon_p^d} \right) \right\} = \\ &= \frac{M}{2} + \frac{M}{2} E \left\{ \cos 2\epsilon_l^d \right\} + 2M \frac{M-1}{2} e^{-\sigma_\epsilon^2} - M^2 e^{-\sigma_\epsilon^2} = \\ &= \frac{M}{2} + \frac{M}{2} \Re (\varphi_\epsilon(2)) - M e^{-\sigma_\epsilon^2} = \frac{M}{2} \left(1 + e^{-2\sigma_\epsilon^2} \right) - M e^{-\sigma_\epsilon^2} \end{aligned} \quad (19)$$

where φ_ϵ is the characteristic function of ϵ_l^d . Similarly,

$$\mu_Y = 0, \quad \sigma_Y^2 = 0.5M - 0.5M e^{-2\sigma_\epsilon^2} \quad (20)$$

Define two standardized RVs, $\tilde{X} \triangleq \frac{1}{\sigma_X} \left(\sum_{l=1}^M \cos \epsilon_l^d \right) - \frac{\mu_X}{\sigma_X}$ and $\tilde{Y} \triangleq \frac{1}{\sigma_Y} \sum_{l=1}^M \sin \epsilon_l^d$. \tilde{J}_a can be represented as a function of \tilde{X}, \tilde{Y} as in (21). The random behavior of \tilde{J}_a is dictated by \tilde{X}^2 and \tilde{Y}^2 which are χ^2 RV with one degree of freedom and by \tilde{X} which is a Normal RV.

$$\tilde{J}_a(\mathbf{w}_{\text{mwf}}^n) = c_1 \cdot \tilde{X}^2 + c_2 \cdot \tilde{Y}^2 + c_3 \cdot \tilde{X} + c_4 \quad (21)$$

where

$$\begin{aligned} c_1 &\triangleq \frac{\sigma_d^6 \sigma_X^2}{(\sigma_n^2 + M\sigma_d^2)^2}, \quad c_2 \triangleq \frac{\sigma_d^6 \sigma_Y^2}{(\sigma_n^2 + M\sigma_d^2)^2} \\ c_3 &\triangleq \frac{2\sigma_d^4 \sigma_X \mu_X}{(\sigma_n^2 + M\sigma_d^2)^2} - \frac{2\sigma_d^4 \sigma_X}{\sigma_n^2 + M\sigma_d^2} \\ c_4 &\triangleq \sigma_d^2 + \frac{\sigma_d^6 \mu_X^2}{(\sigma_n^2 + M\sigma_d^2)^2} - \frac{2\sigma_d^4 \mu_X}{\sigma_n^2 + M\sigma_d^2} + \frac{M\sigma_d^4 \sigma_n^2}{(\sigma_n^2 + M\sigma_d^2)^2} \end{aligned}$$

The expected value and the variance of the \tilde{J}_a can be calculated analytically:

$$E \left\{ c_1 \tilde{X}^2 + c_2 \tilde{Y}^2 + c_3 \tilde{X} + c_4 \right\} = c_1 + c_2 + c_4 \quad (22)$$

$$\text{Var} \left\{ c_1 \tilde{X}^2 + c_2 \tilde{Y}^2 + c_3 \tilde{X} + c_4 \right\} = 2c_1^2 + c_3^2 + 2c_2^2. \quad (23)$$

Deriving an analytical expression for the p.d.f of \tilde{J}_a is a cumbersome task, mainly due to the inherent dependency between \tilde{X}^2 and \tilde{X} . In Sec. 5 we postulate that \tilde{J}_a can be almost accurately described by a Γ RV (for a given mismatch variance σ^2) $f_{J_a}(j_a, \kappa, \theta) = \frac{1}{\theta^\kappa} \frac{1}{\Gamma(\kappa)} j_a^{\kappa-1} e^{-j_a/\theta}$ where κ is the shape parameter and θ is the scale parameter. This postulation is validated empirically by simulations. Assuming for now that \tilde{J}_a is indeed Γ distributed, the expected value

and a variance are given by $\theta\kappa$ and $\theta^2\kappa$, respectively. Comparing these values with (22) and (23), θ and κ can be deduced:

$$\kappa = \frac{(c_1 + c_2 + c_4)^2}{2c_1^2 + c_3^2 + 2c_2^2}, \quad \theta = \frac{2c_1^2 + c_3^2 + 2c_2^2}{c_1 + c_2 + c_4}. \quad (24)$$

We will use the obtained p.d.f to derive a reliability function $R(\sigma^2)$, defined as the probability of the excess MSE due to mismatch conditions not to exceed a pre-defined threshold. Define the excess MSE as the ratio $\text{MSE}_{\text{EX}} \triangleq \tilde{J}_a(\mathbf{w}_{\text{mwf}}^n)/J_{\text{opt}}(\mathbf{w}_{\text{mwf}}^n)$. Based on $\tilde{J}_a(\mathbf{w}_{\text{mwf}}^n)$ description as a Γ RV, and noticing that the nominal MSE is independent of the mismatch parameter σ^2 , $R(\sigma^2)$ is the cumulative density function (CDF) of a Γ RV with shape parameter equal to κ_J , and scale parameter equal to $\frac{1}{J_{\text{opt}}(\mathbf{w}_{\text{mwf}}^n)}\theta_J$:

$$R(\sigma^2) = \Pr(\text{MSE}_{\text{EX}} < T) = \frac{1}{\Gamma(\kappa_J)} \int_0^{\frac{T \cdot J_{\text{opt}}(\mathbf{w}_{\text{mwf}}^n)}{\theta_J}} t^{\kappa_J-1} e^{-t} dt. \quad (25)$$

5. MODEL VERIFICATION

We turn now to the verification of the derived models. For that purpose a simulative benchmark has been designed. Arrays with $M = 10$ sensors, $\Delta_x = \lambda/2$ and $\Delta_y = 0$ are used. Desired and interfering sources are arriving from the far-field, with angles of arrival equal to $\theta_d = 90^\circ$ and $\theta_i = 120^\circ$, respectively and frequency 1500 Hz. A sensor noise is added to the received signals, with signal to noise ratio (SNR) 40 dB, and signal to interference ratio (SIR) 0 dB. The MWF beamformer (2), $\mathbf{w}_{\text{mwf}}^n$, is designed with nominal conditions (1a) and applied to actual signals (1b). For each σ^2 , the average performance of the $\mathbf{w}_{\text{mwf}}^n$, defined as $E_{\text{emp}} = E_t \{ |s_d(l) - (\mathbf{w}_{\text{mwf}}^n)^H \mathbf{z}_a(l)|^2 | \mathbf{a}_d^d, \mathbf{a}_a^i \}$, is calculated, where $E_t(\cdot)$ stands for time averaging. Both the empirical error and the approximated MSE are then averaged using 50,000 Monte-Carlo simulations, randomized over the actual signals. In Fig. 1 $\tilde{J}_a(\mathbf{w}_{\text{mwf}}^n)$ is compared with \bar{E}_{emp} . It is clearly depicted that $\tilde{J}_a(\mathbf{w}_{\text{mwf}}^n)$ is well within $\pm\text{STD}$ of \bar{E}_{emp} . Our main interest in this

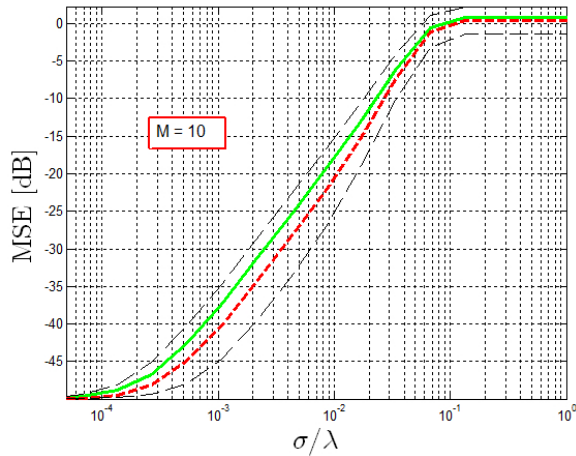


Fig. 1: \bar{E}_{emp} vs. $\tilde{J}_a(\mathbf{w}_{\text{mwf}}^n)$.

work is to parameterize the p.d.f of E_{emp} by using the statistics of $\tilde{J}_a(\mathbf{w}_{\text{mwf}}^n)$. To demonstrate the relation between the distributions

of E_{emp} and $\tilde{J}_a(\mathbf{w}_{\text{mwf}}^n)$, a Quantile-Quantile plot of the two distributions is depicted in Fig. 2a. A clear match is evident. Moreover, E_{emp} histogram is almost accurately described by a Γ p.d.f as can be deduced from Fig. 2b. To further validate the later argument, we found the Maximum Likelihood parameters of the Γ p.d.f, κ_{ML} and θ_{ML} , that fit the E_{emp} histogram for each value of σ^2 . The resulting Γ p.d.f.s are depicted together with E_{emp} histograms in Fig. 2b. In addition, a comparison between κ_{ML} and θ_{ML} and the theoretically obtained approximated values κ_J and θ_J (24) is given in Fig. 3, demonstrating good correspondence. Finally, in Fig. 4 the

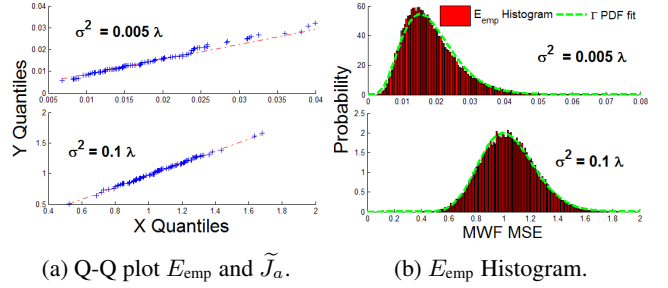


Fig. 2: E_{emp} and $\tilde{J}_a(\mathbf{w}_{\text{mwf}}^n)$ Statistics.

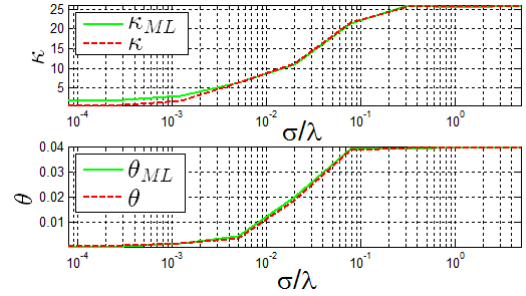


Fig. 3: Γ PDF parameters.

reliability function is presented for $M = 10$, and different σ^2 .

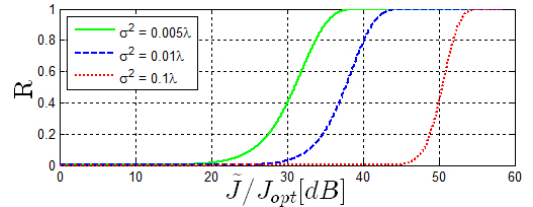


Fig. 4: Reliability functions.

6. DISCUSSION

A randomly positioned microphone array was considered in this work. We analyze the free-field scenario, with one desired source, and one interfering source impinging on a planar microphone array. A reliability function for predicting the MWF residual error for a given uncertainty in sensors locations is derived and validated by simulations. The reliability function provides a powerful tool for designing the beamformer under mismatch conditions.

7. REFERENCES

- [1] Harry L Van Trees, *Detection, Estimation, and Modulation Theory, Optimum Array Processing*, John Wiley & Sons, 2004.
- [2] Sharon Gannot, David Burshtein, and Ehud Weinstein, "Signal enhancement using beamforming and nonstationarity with applications to speech," *IEEE Transactions on, Signal Processing*, vol. 49, no. 8, pp. 1614–1626, 2001.
- [3] Barry D Van Veen and Kevin M Buckley, "Beamforming: A versatile approach to spatial filtering," *ASSP Magazine, IEEE*, vol. 5, no. 2, pp. 4–24, 1988.
- [4] Henry Cox, R Zeskind, and Theo Kooij, "Practical supergain," *IEEE Transactions on, Acoustics, Speech and Signal Processing*, vol. 34, no. 3, pp. 393–398, 1986.
- [5] Dovid Levin, Emanuel AP Habets, and Sharon Gannot, "Robust beamforming using sensors with nonidentical directivity pattern," in *Proc. 38th IEEE Int. Conf. Acoust. Speech, Signal Process. (ICASSP13)*, Vancouver, 2013, IEEE.
- [6] Y Lo, "A mathematical theory of antenna arrays with randomly spaced elements," *IEEE Transactions on, Antennas and Propagation*, vol. 12, no. 3, pp. 257–268, 1964.
- [7] Shmulik Markovich-Golan, Sharon Gannot, and Israel Cohen, "Performance of the SDW-MWF with randomly located microphones in a reverberant enclosure," *IEEE Transactions on, Audio, Speech, and Language Processing*, vol. 21, no. 7, pp. 1513–1523, 2013.
- [8] Simon Doclo and Marc Moonen, "Superdirective beamforming robust against microphone mismatch," *IEEE Transactions on, Audio, Speech, and Language Processing*, vol. 15, no. 2, pp. 617–631, 2007.
- [9] Simon Doclo and Marc Moonen, "Design of broadband beamformers robust against gain and phase errors in the microphone array characteristics," *IEEE Transactions on, Signal Processing*, vol. 51, no. 10, pp. 2511–2526, 2003.
- [10] Shmulik Markovich Golan, Sharon Gannot, and Israel Cohen, "Performance analysis of a randomly spaced wireless microphone array," in *IEEE International Conference on Acoustics, Speech and Signal Processing (ICASSP), 2011*. IEEE, 2011, pp. 121–124.